⦿ Technical Paper

Evaluaton of Fatigue Crack Propagation Rate Using Parameter of Fatigue Strain Intensity Factor +

Young-Chul Park,* Sae-Wook Oh,* Chung-Weon Hue,**
Hyuk-Dong Kwon** and Kwang-Young Kim***
(*Received Nov.* 16, 1991)

피로변형율확대계수 △A를 이용한 피로크랙 전파속도 평가

박 영 철 · 오 세 욱 · 허 정 원 · 권 혁 동 · 김 영 광

Key Words : Crack Tip(균열선단), Fatigue Strain Intensity Factor(피로변형율 확대계수), Fatigue Crack Propagation Rate(피로크랙 전파속도), Fine Dot Grid Strain Measurement Method(미소원형격자 변형율 측정법)

초 록

본 연구는 피로수명 평가를 위한 새로운 파괴역학적 parameter의 확립에 관한 연구이다. 실질적으로 피로파괴가 일어나는 피로 균열선단의 국소영역에서 변형분포를 미소원형격자 측정법을 이용하여 실험적으로 명확히 밝혀내었다. 그리고 이 결과를 기초로 하여 국소피로 변형율장을 대표할 수 있는 피로변형율 확대계수 △A를 제안하였다.
또한 새로운 parameter △A의 유효성을 여러 피로조건에서 검토한 결과, 균열선단 국소 영역에서 피로 변형율 확대계수 △A에 의하여 피로 균열전파 속도평가를 일의적으로 나타낼 수 있음을 확인하였다.

1. Introduction

Fatigue fracture is a very localized phenomenon. Therefore, study on the stress and the deformation of the material near the crack tip is a prerequisite to solving the fatigue fracture problems.

In the studies of this field, many theoretical results have been reported by using the fracture mechanics theory and the finite element method[1-3]. However the theoretical solution about the state of deformation near crack tip is very difficult to obtain due to its inherent matematical complexi-

+ Presented at Beijing, China, Oct. 8~10, APCS-91(Asian-Pacific Congress on Strength Evaluation)
* Member, Dong-A University
** Member, Graduate Student of Dong-A University
*** Member, Korea Institute of Machinery & Metals

ties. Therefore, theoretical solution can be only obtained under the simple assumptions such as homogeneous isotropic elastic material or perfectly plastic material. Since the actual material behaviour near the crack tip is, however, far from such simple assumptions, it has been pointed out that the state of deformation near the crack tip could not be obtained easily by a thoretical analysis. For this reason, it has been argued that the accurate experimental analysis about the state of deformation near the crack tip is necessary to solve fatigue fracture problems. However, it is very difficult to measure the local cyclic strain near the crack tip by the conventional experimental methods, because the strain near the crack tip is very large and also its distribution is steep. Therefore, many efforts have been made, in the studies of this field but only a few results have been reported[4)~6)]

In this study, the local cyclic strain distribution near the crack tip was investigated by the Fine Dot Grid Measurement Method which is a newly developed method to resolve these experimental difficulties. As a result, it was found that the shape of local cyclic strain distribution near the crack tip was not altered by the applied cyclic load level or by the material. From this result, the parameter of local cyclic strain distribution $\triangle$A, which characterizes the local cyclic strain field, could be proposed. In addition, the parameter $\triangle$ A was applied to fatigue crack propagation. As a aresult, the fatigue crack propagaion rate could be estimated by a parameter $\triangle$A.

2. Experimental Procedures

The test materials used in this study were Ni−Cr alloy steel and 2024−T3 aluminum alloy.

Table 1 Chemical compostion of materials

Al 2024−T3 (wt.%)

Si	Fe	Cu	Mn	Mg	Zn	Ti
0.07	0.14	4.06	6.67	1.27	0.01	0.06

SNC 631 (wt.%)

C	Si	Mn	P	S	Cu	Ni	Cr
0.29	0.22	0.51	0.02	0.02	0.06	2.59	0.70

The chemical compositions of the materials are given in Table 1. 2024−T3 Aluminun alloy was used as−received condition, but the Ni−Cr alloy steel was heat−treated to obtain various mechanical properties.

The heat-treatment conditions and the obtained mechanical properties of the materials are given in Table 2.

The compact tension specimen shown in Fig. 1 was used in this study. A fatigue pre-crack was introduced to be length of 0.5 W under small cyclic loading by using servohydraulic fatigue test machine (INSTRON 1331, 10 *tonf.*)

The dot type fine grid pattern at the crack tip (array of fine dots, 25.4 *μm* pitch and 5*μm* diameter), which was used for measuring the cyclic strain near the crack tip, was engraved by a technique of electropolishing on the specimen surface as shown in Fig. 2. Aconstant amplitude load con-

Table 2 Heat treatment conditions of Ni−Cr alloy and the obtained meachanical properties of materials

	Heat treatment condition			Mechanical properities		
	Quenching	Tempering	Aging	Y.S(*MPa*)	T.S(*MPa*)	Elongation (%)
SNC631−A	1050℃, O.Q	600℃, O.C	480℃,100h. A. C	824.0	915.2	19.4
SNC631−B	1050℃, O.C	600℃, O.C		823.8	890.5	20.0
SNC631−C	1050℃, O.Q	200℃, O.C		1400.2	1723.5	12.6
Al 2024−T3	As received			460.1	500.2	13.5

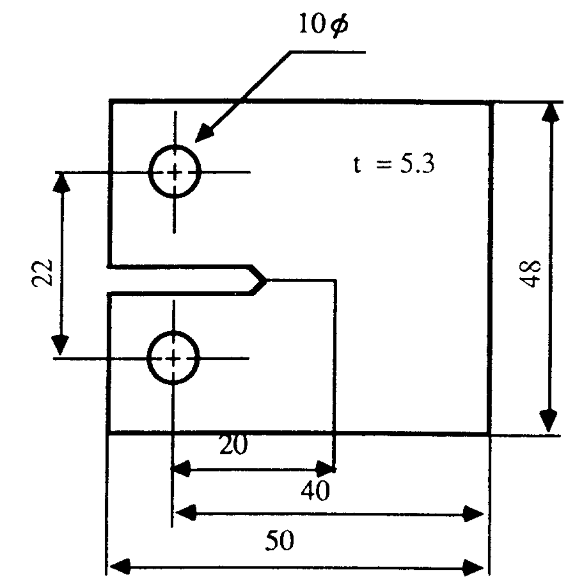

Fig. 1 Specimen geometry and dimensions (*mm*)

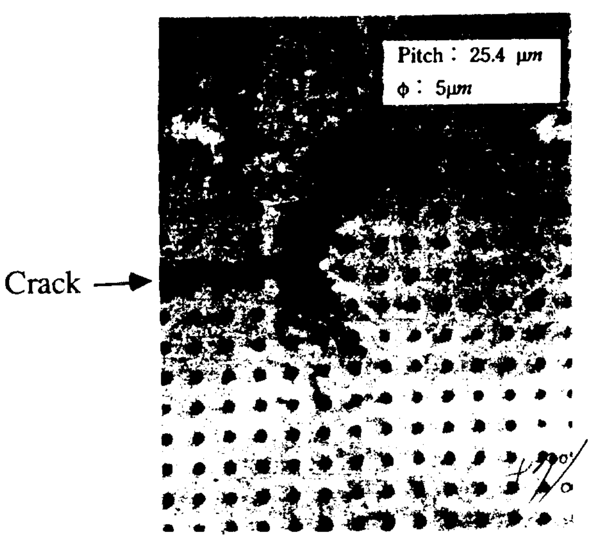

Fig. 2 Photograph of fine dot grid

trol test was performed in the sinusoidal waveform in air at room temperature.

Simultaneously, the state of deformation of the fine grids near the crack tip was directly photographed through the optical system. From the negative film, the cyclic change of the local strain distribution was measured by using the Fine Dot Grid Measurement Method.

Fig. 3 shows the image processing system for the Fine Dot Grid Measurement Method. The coordinates (X and Y) of each dot were measured directly from photographed negative film by using the image processing system, and then the displacement could be obtained by the comparison of the coordinates of the deformed grid with those of the undeformed grid at the beginning of the fatigue test. The image processing system for fine grid, and the calculation procedure for strains can be found in Ref(7).

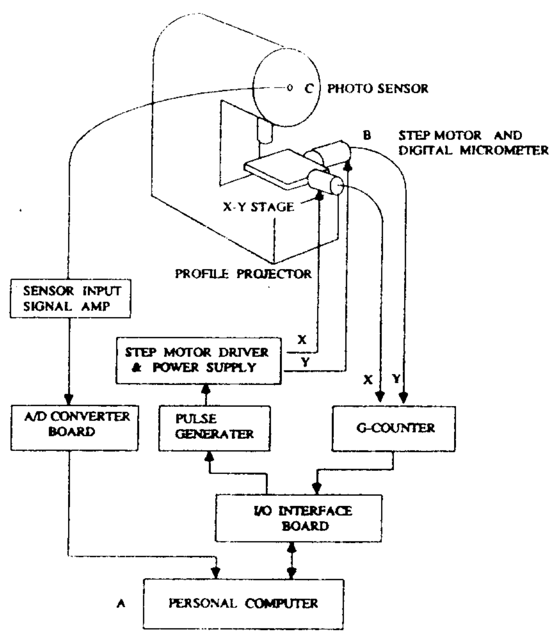

Fig. 3 Schematic diagram of the image processing system

3. Results and Discussion

3. 1 Local cyclic strain distribution

The local cyclic strain distribution near the crack tip was measured by the fine dot grid measurement method for various specimens.

Fig. 4 shows the typical example of the equivalent cyclic strain distribution near a crack tip. As shown in Fig. 4, the direction of the maximum

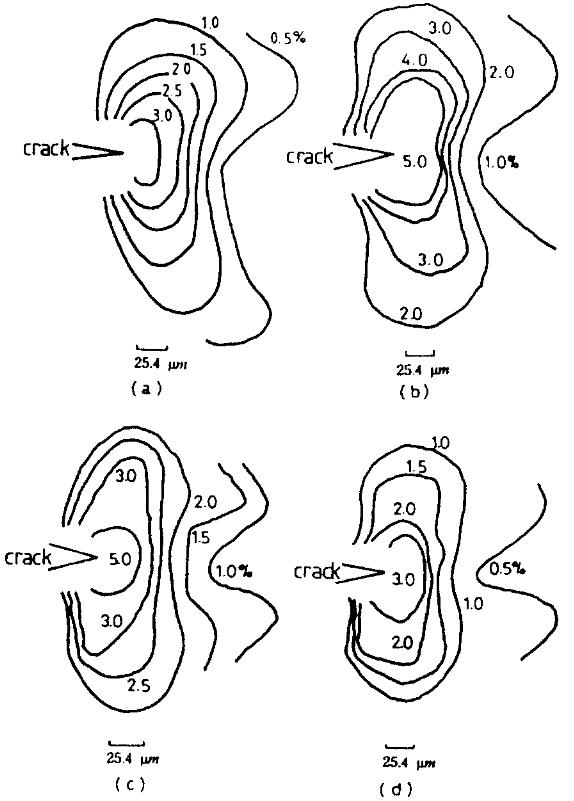

(a)	(b)
SNC 631−A	SNC 631−B
△K = 34.8, N = 11 *MPa* *Cycles*	△K = 47.4, N = 10 *MPa* *Cycles*
(c)	(d)
SNC 631−C	Al 2024−T3
△K = 47.4, N = 10 *MPa* *Cycles*	△K = 34.8, N = 11 *MPa* *Cycles*

Fig. 4 Cyclic strain distribution near a crack tip

cyclic strain distribution was inclined toward 70°~80° from the crack propagation direction without respect to materials and cyclic loading, and the magnititude of the cyclic strain distribution was varied depending on the applied load level and the material. But the shape of local strain distribution did not change so much. From these results, authors considered that the cyclic strain field near the crack tip could be characterized by the new single parameter, and that the parameter could be derived from these experimental data for cyclic starain distribution near the crack tip. Generally, in the linear elastic fracture mechanics, the stress field near the crack tip is characterized by the stress intensity factor K, as in Eq(1).

$$\delta(r, \quad \theta) = K \cdot f(\theta) \cdot r^{-1/2} \quad \cdots\cdots\cdots\cdots\cdots\cdots \quad (1)$$

Similarly in this study, it was considered that cyclic strain distribution near the crack tip could be characterized by the parameter △A as in Eq. (2) if the cyclic strain always has linear relation to the distance from the crack tip(r) and the angle (θ).

$$\triangle\varepsilon(r, \theta) = \triangle A \cdot f(\theta) \cdot f(r) \quad \cdots\cdots\cdots\cdots \quad (2)$$

For this reason, the relationship between △ε and r, and between △ε and θ were investigated experimentally in the following.

Fig. 5 shows the relationship between the equivalent cyclic strain and the angle. The equivalent cyclic strains were obtained on a circle (radius r = 50.8 ㎛) around the crack tip. As shown in this figure, all data points lay nearly on a single symmetric curve, independently of the cyclic load levels, the number of cycles and the materials. From these results, the angular dependence of the equivalent cyclic strain is expressed in Eq (3).

$$f(\theta) = \cos(\theta/2) \cdot (1+3/2\sin^2\theta) \quad \cdots\cdots\cdots \quad (3)$$

Fig. 6 shows a typical example of the relationship between the normalized equivalent cyclic strain and the distance from the crack tip. All of the points were found to fall on a simple line. It could be seen that the relation between $\triangle\varepsilon_{eq}$ and was rexpressed by a line with the slope of −1 on a log − log plot.

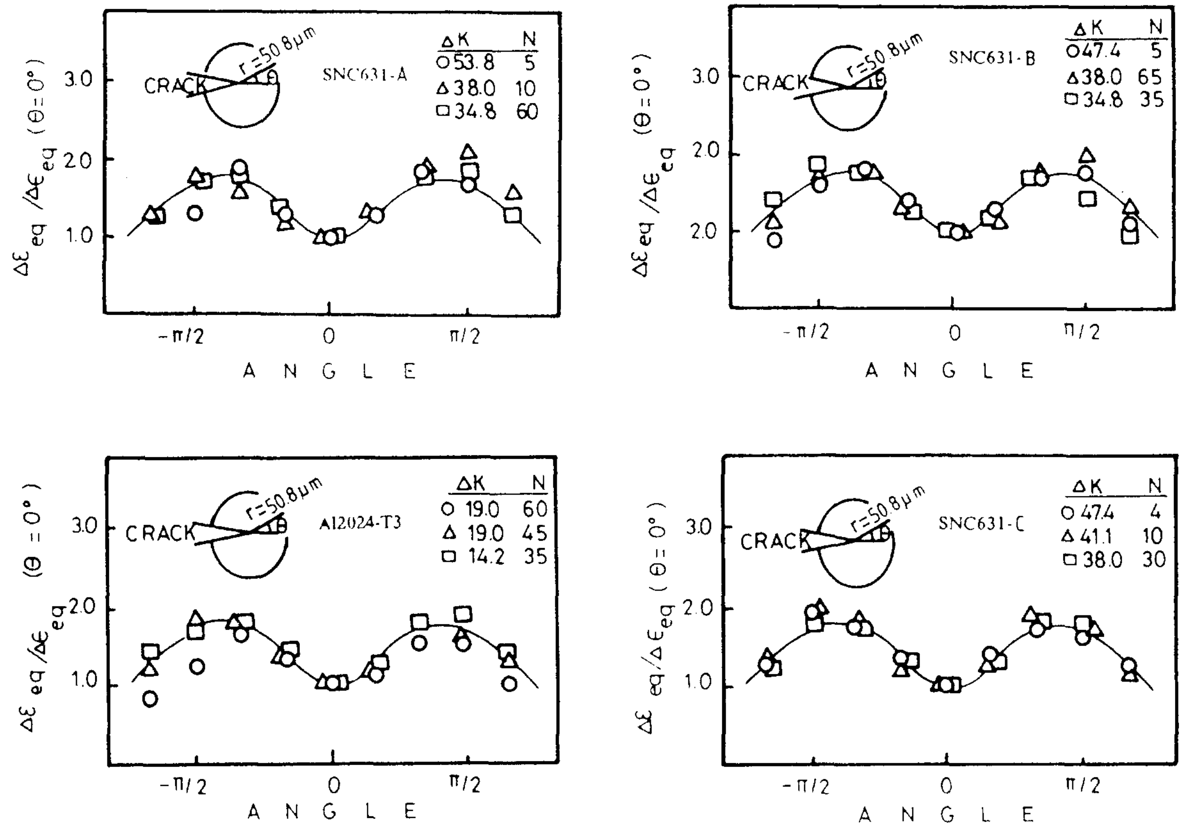

Fig. 5 Angular dependence of the equivalent cyclic strain at r=50.8μm

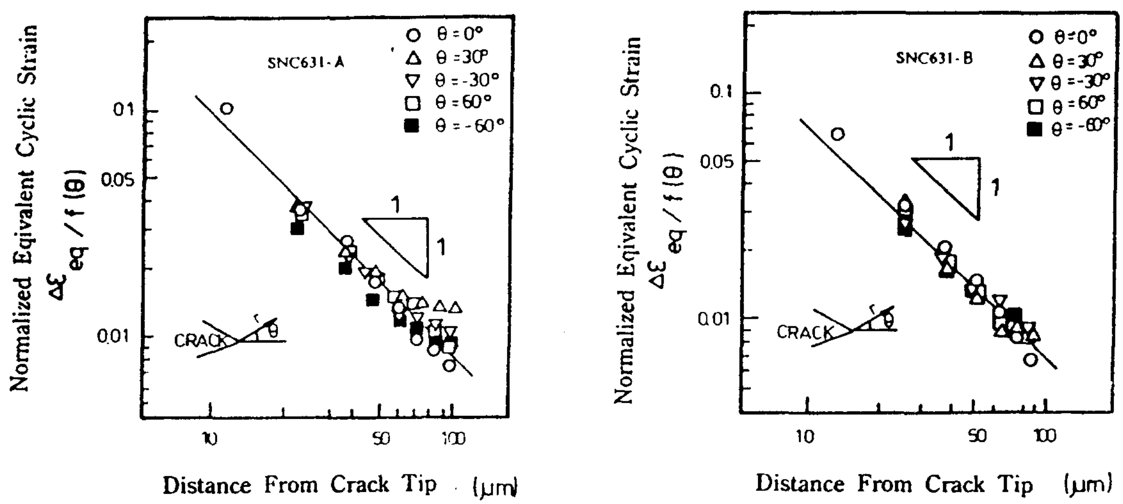

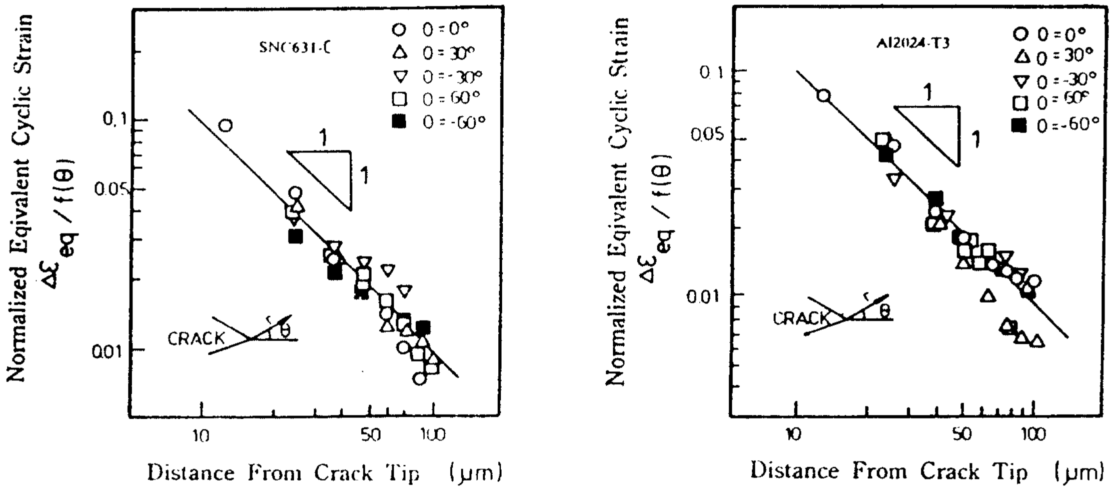

Fig. 6 Relationship between the normarlized equivalent cyclic strain and the distance from the crack tip

From the results of Fig. 5 and 6, the equivalent cyclic strain distribution near the crack tip would be expressed by a single fomulation as follows,

$$\triangle\varepsilon_{eq}(r,\ \theta) = \triangle A \cdot f(\theta) \cdot r^{-1} \quad \cdots\cdots\cdots\cdots\cdots \ (4)$$

where (θ) is a function of angle and $\triangle A$ is a constant.

Consequently from Eq(4), it was thought that the cyclic strain distribution near a crack tip could be characterized by the parameter $\triangle A$.

3. 2 Application of parametr △A to fatigue crack propagation

Fig. 7 shows the relationships between da/dN and $\triangle K$ with various R values for Al 2024−T3. As shown in this figure, fatigue propagation rate da/dN was increased according to stress ratio R. These plots showed that the log−log relation was a single straight line varied with R. These data points distribution band varied systematically with stress ratio R, that is the higher the stress ratio, the higher the rate of fatigue crack growth for given value of $\triangle K$. And it could be also noted that the da/dN was varied with R even so the

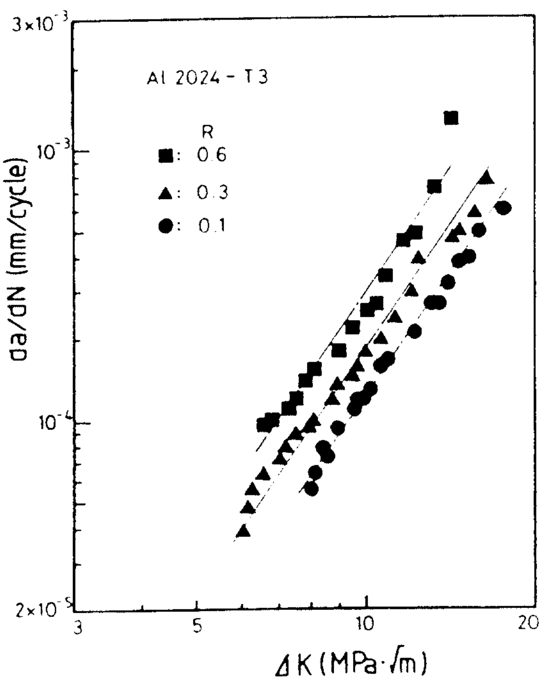

Fig. 7 Relationship between da/dN and $\triangle K$ for various R values

same material.

Fig. 8 shows the relationship between da/dN and $\triangle$Keff for various R value. As shown in Fig. 7, the effect of stress ratio R was not nearly va-

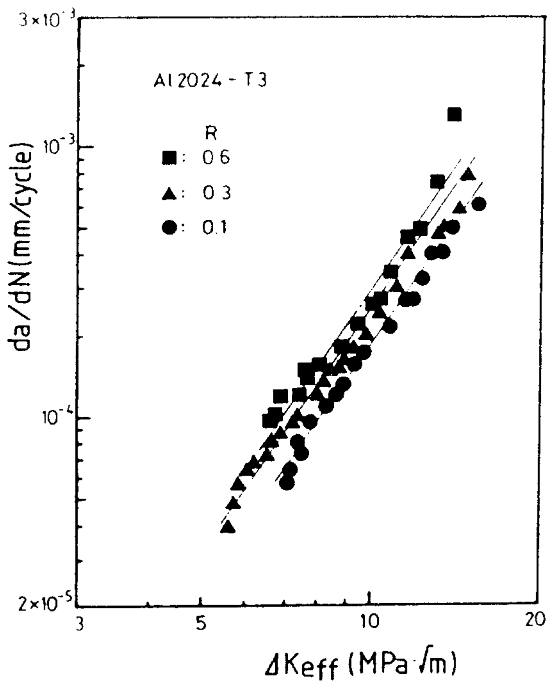

Fig. 8 Relationship between da/dN and △Keff for various R values

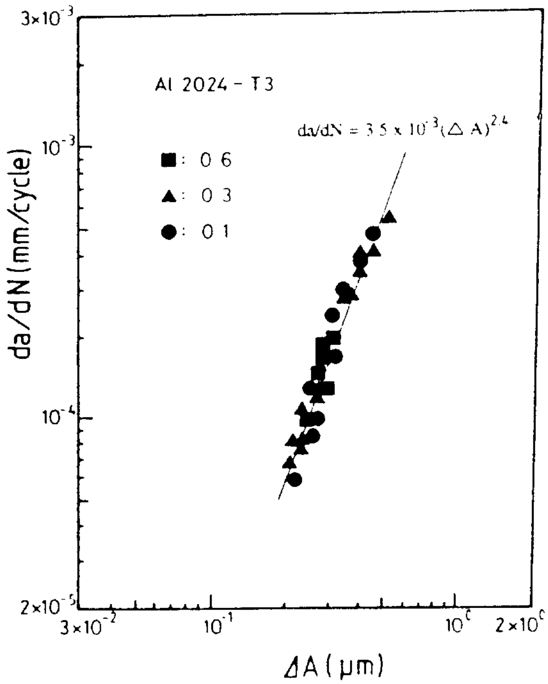

Fig. 9 Relationship between da/dN and △A for various R values

ried. Effective stress intensity factor range (△Keff)showed more increased tendency than stress intensity factor range (△K) when R was 0.1 and 0.3. Also data point distribution band was become narrowed. In the case of aluminum alloy, these phenomea was different stress ratio (R) arranged in △(K−da/dN relation was decreased and eliminated by mechanical effectivensess of △Keff[9~10]. The same phenomea was reported[11] that were occurred in other alunium alloy besides materials used in this experiment.

Fig. 9 shows the relationship between da/dN and △A for various R value, where △A was called cyclic strain intensity facter. As shown in this figure, all data points were plotted on a single line independently of R value. The following equation was found to fit the experimented data.

$$da/dN = 3.5\times 10^{-3} \quad (\triangle A)^{2.4} \cdots\cdots\cdots\cdots\cdots \quad (5)$$

Various quantitative models have been proposed to explain the emmpirical relations between crack growth rate and stress intensity factor range. One of most equation widely accepted was the Paris−Erdogam[8] fatigue crack growth law, was

$$da/dN = C(\triangle K)^{n} \quad \cdots\cdots\cdots\cdots\cdots\cdots\cdots\cdots\cdots \quad (2)$$

By using Eq. (6), table 3 was indicated results to be calculated each data of Fig. 7, 8. Fig. 7 and 8 have different band wide and were showed 3 linear line with same slope. However, Fig. 9 arranged by △A was drived into a single line regardless of stress ratio R (Eq. (6)). As these experimental results, it was noticed that the fatigue crack propagation rate could be evaluated by the parameter △A. Therefore, parameter △A was proposed as effective parameter for the fatigue crack propagation rate.

Table 3 Calculation of da/dN with various R values in Fig. 7, 8

R	△K	△Keff	n
	C		
0.1	2.091×10^{-7}	2.944×10^{-7}	2.6
0.3	3.866×10^{-7}	4.792×10^{-7}	2.6
0.6	5.523×10^{-7}	2.523×10^{-7}	2.6
$da/dN = C\left(\begin{matrix}\triangle K \\ \triangle K_{eff}\end{matrix}\right)^n$			

3. 3 Simple calculating method for parameter △A form △ ε_Φ

From the above results, it was found that the parameter △A was very effective parameter for the fatigue crack progagation rate. However, in actual, it was very troublesome to determine the parameter △A by the experimental method. If the parameter △A could be calculated by simple method, it would be very useful for a quantitative prediction of fatigue crack propagation rate.

Fig. 10 shows the relationship between △A and ε_Φ at various measuring point. In this study, $\triangle\varepsilon_\Phi$ is the local cyclic strain measured along the perpendicular direction to the crack growth direction at the various backward position from the crack tip as the figure. As shown in this figure, the relationship between △A and $\triangle\varepsilon_\Phi$ were plotted on a single line regardless of the materials and the loa-

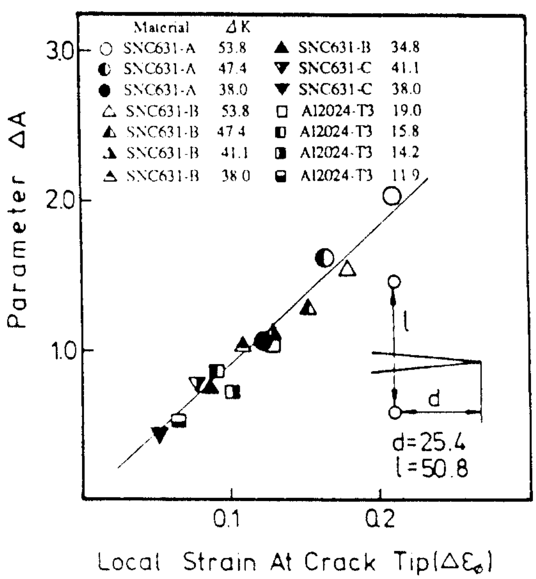

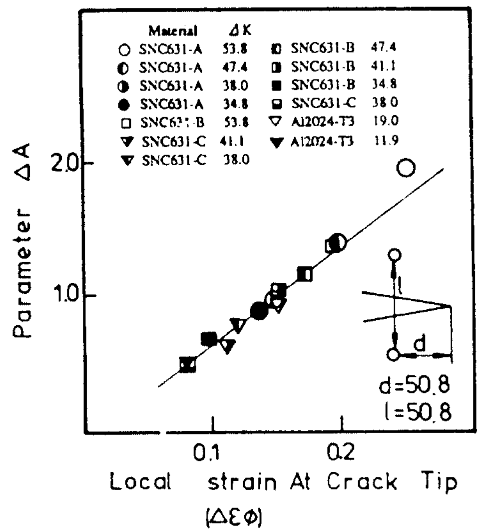

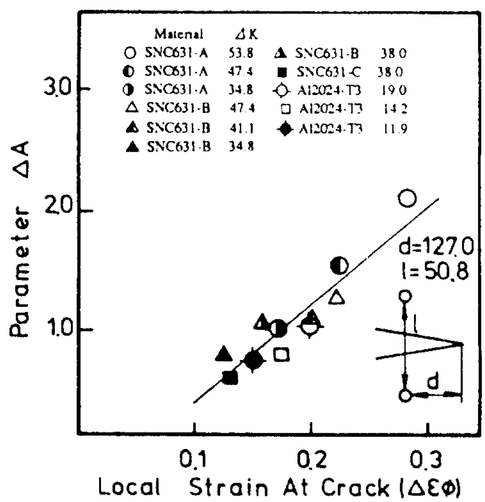

Fig. 10 Relationship between fatigue strain intensity factor(△A) and local cyclic strain at crack tip ($\triangle\varepsilon_\Phi$) at various measure points

ding condtion within d = 50.8 μm. However, this linear relationship did not hold for d = 127 μm.

Figure 11 shows the relationship between $\triangle A$ and $\triangle \varepsilon_{\phi}$ with various gage length(ℓ). It was found that the relationship between $\triangle A$ and $\triangle \varepsilon_{\phi}$ were expressed by a single line for the same value of gage length regardless of the materials and the loading condition

From the above results, the relationship between $\triangle A$ and $\triangle \varepsilon_{\phi}$ could be expressed as Eq.(7) within the heavily deformed region near the crack tip ($d \leq 50.8 \mu m$), where α is proportional constant depending on a gage lenth

$$\triangle A = \alpha \cdot \triangle \varepsilon_{\phi} \quad \cdots\cdots\cdots\cdots (2)$$

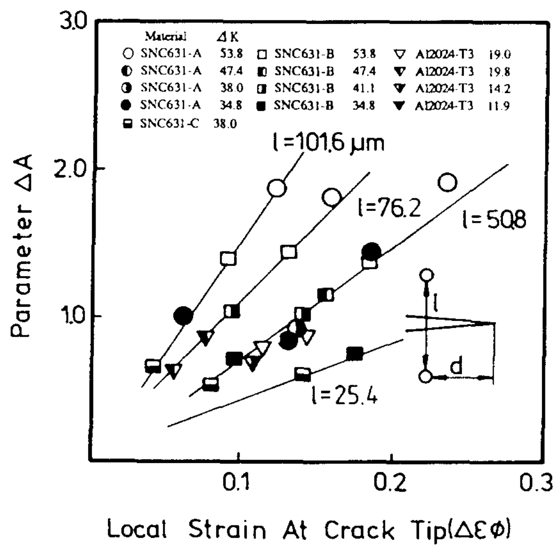

Fig. 11 Relationship between parameter ($\triangle A$) and local cyclic strain at crack tip ($\triangle \varepsilon_{\phi}$) for various gage length (d = 50.8 μm)

4. Conclusions

The local cyclic strain distribution near crack tip was investigated by the fine dot grid measurement method.

1) The distribution of local cyclic strain near the crack tip could be expressed by eq(3). Therefore, the local cyclic strain field dould be characterized by the parameter $\triangle A$

2) The fatigue crack propagation rate was expressed linealy by parameter $\triangle A$ for the wide range of the crack propagation rate without R effect. So, parameter $\triangle A$ could be considered as useful parameter for fatigue crack propagation rate.

3) The simple calculating method for parameter $\triangle A$ from $\triangle \varepsilon_{\phi}$ was proposed as follows ;

$$\triangle A = \alpha \cdot \triangle \varepsilon_{\phi}$$

References

1) Rise, J.R., ASTM STP 415, pp.247~309, 1967
2) Rice, J. R. and G. E. Rosengen, J. Mech. Phys. Solids, pp. 1~12, 1968
3) Hu, Wan-liang and H. W. Liu, ASTM STP 601, pp. 522-534
4) Davidson, D. L. and J. L., Lankford Fatigue of Engng Mater and Structure 3, pp. 289-303
5) Ohta. A. M. Kosuge. ans E., Sasaki. Int. J. Fracture 13, pp. 280~300, 1977.
6) Shimada, H. and Y., Furuya. Exp. Mech. 21, pp. 423~428, 1981
7) Park, Y. C., S. W. Oh, and K. Y. Kim, KSME, 15, 1, pp. 290~217, 1991
8) Paris, D. C. and F., Erdogan. J. Basic Engng, Transactions ASME, Series D. 85, pp. 528~534, 1963
9) Walker, K., "The Effect of Stress Rate during Crack Propagation and Fatigue for 2024-T3 and 7075-T_6 Alluminum, Effects of Environment and Complex Load History On Fatigue Life, ASTM STP 462, pp. 1~14, 1970
10) Omer, G. Bilir and Metin Harun., "Effect of Stress Ratio on the Rate of Growth of Fatigue Cracks in 1100 Al-Allloy," Engineering Fracture Mechanics, Vol 37, No, 6, pp. 1203~1206, 1990
11) Srivastava. Y. P., and S. B. L., Garg "Influence of R on Effective Stress Range Ratio and Crack Growth," Engineering Fracture Mechanics, Vol. 22, pp. 915~926, 1985